NERC Geophysical Equipment Facility loans 910 & 928: "Subsurface density structure associated with an active intrusion in the central Andes – Bolivia." SCIENTIFIC REPORT

Joachim Gottsmann (PI) and Rodrigo del Potro (PDRA)

School of Earth Sciences, University of Bristol, BS8 1RJ, Bristol. Tel. (0117) 9545422, fax (0117) 9253385, e-mail j.gottsmann@bristol.ac.uk

Abstract

Dual frequency GPS and gravity measurements were performed during two survey campaigns in southern Bolivia in 2010 using GNSS equipment provided by the NERC GEF facility in Edinburgh. The survey area is located around Uturuncu volcano, in Southern Bolivia. The aims of the campaigns were to determine the local gravity anomaly. In addition, a joint GPS/microgravity network was installed for repeat measurements in the future. These dynamic data will be used to constrain the evolution of mass and density changes beneath Uturuncu. The GEF loans supplement research in the area as part of the NERC standard grant NE/G01843X/1. Both campaigns proved successful in achieving the aim of the surveys and uncertainties in the post-processing of the data were lower than expected. The local gravity anomaly map shows several local minima, related to Quaternary stratovolcanoes, and no clear correlation to the large Neogene ignimbrite systems. Our first interpretations point to the presence of partial melt beneath the most recently active volcanoes.

1. Introduction

Almost two decades of ground uplift centred on Uturuncu volcano, in southern Bolivia, have been identified in the past using InSAR techniques [Pritchard and Simmons 2002]. The 70 km-wide footprint of the identified deformation anomaly constrains the source of this deformation at 15 to 20 km depth in the middle crust; in a region that other regional geophysical data indicate is the top of a thick region of hot partially molten rock known as the Altiplano-Puna Magma Body (APMB) [Schilling et al., 2006 and references therein]. The objective of NERC standard grant NE/G01843X/1, which GEF loans 910 and 928 supplement, is to document the dynamics and the characteristics of the intrusion. This requires knowledge of the sub-surface architecture and regional structures to understand the spatio-temporal evolution of the system. The approach followed during the first two of several future geodetic campaigns was to perform combined GPS and gravity surveys.

2. Geologic setting (including field survey site location map)

Uturuncu is a large stratovolcano in Southern Bolivia that towers at 6008 m asl above the Altiplano (around 4100 m). It is part of the Altiplano-Puna Volcanic Province (APVC), a region of high volcanism dominated by large Neogene ignimbrites that were erupted during a so-called "flare-up" period [Salisbury et al., 2010], which sits on top of the aforementioned APMB. Uturuncu is part of the post-flair-up activity and it last erupted 270 ka ago [Sparks et al., 2003]. Products from Uturuncu are mostly dacitic domes and lavas with andesitic enclaves. Studies in the area have focussed on a more regional scale and, at present, little is known about the magma storage and plumbing systems. Yet, InSAR data suggests that magma may be accumulating beneath Uturuncu.

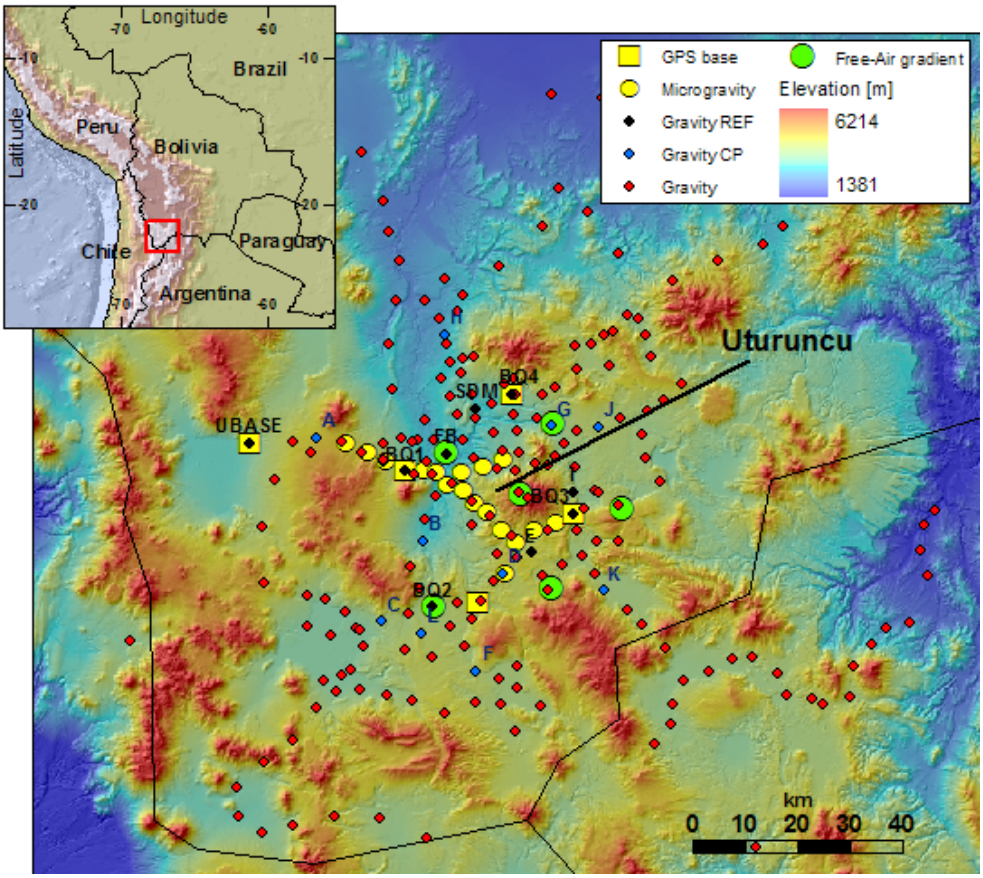

Figure 1. Map of the surveys

3. Survey setup

3.1. Static survey

The new local gravity anomaly survey covers an area of 5000 km^2 in the South Lípez region in Southern Bolivia (Figure 1). The new survey comprised the co-location of LEICA 1200 dual frequency GPS and SCINTREX CG5 Autograv spring gravimeter at 141 new locations with average spacing of ~5 km at elevations between 4000 and 6000 m (Figure 1). Benchmark location choice took into account: survey areal coverage, minimal near-field terrain effect and good accessibility (for short measurement loop times). In the absence of absolute gravity benchmarks, gravity data are relative to an arbitrary gravity reference (UBAS) located about 35 km W of Uturuncu. Elevation data is obtained through static differential GPS. Gravity data is obtained through loops that start and finish at one of the eight reference (REF) or nine control points (CP), installed to counter a decrease in data precision as a function of distance from UBAS. This is particularly important for the gravity survey, as the quality of the data deteriorates with increasing length of survey loops in the rough terrain of the Altiplano. The CP and REF were linked to UBAS at the end of the survey. Monumentation for the REF, where repeated measurements were required, were built using 40 cm-long masts, which we installed by drilling and concreting into bedrock to mount the GPS antennas. The gravimeter was located precisely at the same position at the REF to minimize positioning errors. At each benchmark gravity data recorded at 6 Hz were averaged over two 60-second periods and GPS readings were set at 3 second epochs for measurement times of approximately

1-minute per kilometre of baseline. Additionally, seven local vertical gravity gradients or free-air gradients (VGG) were determined at six different locations, where gravity was repeatedly measured at two different elevations over the same point using a vertically extendable tripod.

3.2. Dynamic (time-lapse) microgravity

Microgravity measurements obtain a significantly higher precision, to those of the static gravity survey, through precise repeat measurements and loops from the base to any given benchmark (between 3 and 9 times for each campaign). Moreover, measurement uncertainties are minimised by averaging 6 Hz gravity data over five 60-second periods. GPS monuments are built following the UNAVCO single-mast guidelines: a 20 cm-long pin is epoxied to a rock outcrop and a 50 cm-long mast with a rotation adaptor, where the GPS antenna is set, is screwed to the pin. The antenna is therefore always at the same height and has the same orientation. Similarly, the gravimeter is always set on the same position and elevation. GPS data is improved by using a more complex external reference frame comprising three cGPS and three NERC-GEF GPS set to record continuously during the length of the campaign. GPS data is further enhanced by recording simultaneously at the bases and the rovers for a minimum of 18 hours overnight. Repeat measurements at certain stations provided us with repeatability errors for the measurements.

Ocean loading and diurnal pressure variation effects were studied through continuous gravity observation, performed by an automated Burris gravity meter (B-28) in 2010 over a 7-day period at Quetena Chico village (22.192ºS, 67.34ºW), near the centroid of the survey. The time series revealed a ±3 μGal and ±2 μGal uncertainty for ocean loading over semidiurnal frequencies and for pressure admittance over diurnal frequencies, respectively. In order to minimise their effect, most loops were kept to less than six hours and a white noise constant of 1 μGal was introduced to the data set.

4. Data quality

De-tided gravity data for each rover within each loop has an error that is a compound of: measurement uncertainty (at the base and at the rover) and loop closure (difference in repeat measurement at the base, which results from unaccounted drift and possible tares during the loop). Measurement uncertainty ranged, at one sigma, between 0 and ±3 μGal per station whereas loop closure varied greatly depending on the length of the loop and the roughness of the terrain. When linking REF and CP, and in the time-lapse survey these were minimised by reoccupying the benchmarks during different loops. The weighted average and standard deviation of the repeat baselines were propagated to UBAS.

In the static survey, relative to UBAS, gravity uncertainty at one sigma ranges ±2 to ±92 μGal with an average of ±41 μGal. Repeat measurements at nine CP were always within the uncertainty of the data. Further quality control was introduced by performing repeat REF links forming loops: for all cases, the difference in loop closure was smaller than the uncertainty. The absolute position of BQ1 was calculated as the weighted average of 8-hour RINEX solutions from NASA-JPL's Automatic Precise Positioning Service (APPS). The calculated standard deviation is ±0.5 cm. Relative to it GPS positions are post-processed using Leica Geo Office, with precise ephemeris and with single solutions for all baselines, when applicable. At one sigma, 85% of measurements had an uncertainty

<±2.5, 13.2% were between ±2.5 and ±5 cm, with the remainder 1.7% having an uncertainty >±5 cm. GPS repeatability was tested by re-measuring seven control points. Maximum differences in any component were less than the associated uncertainties.

Errors in determining the local vertical gravity or free-air gradient (VGG) arise mostly from measurement uncertainty, most significantly from measuring atop a 1 m mast held by a bipod. Still, overall uncertainties for the free-air gradient measurements, at one sigma, were <±10 μGal/m.

The uncertainty of microgravity benchmarks, at one sigma, propagated to UBAS, were <±6 μGal for the baseline survey, which was later improved to <±3 μGal for the first campaign, by increasing the number of loops to a given benchmark. GPS data was processed using GAMIT-GLOBK where position repeatability was < 0.6 cm and a velocity field was obtained. Moreover, control measurements show a repeatability of 0.8 cm.

5. Processing and modelling

The theoretical Earth model by Wahr, Dehant and Defraigne [1999] is used to de-tide all gravity data. Standard methodologies in gravimetric data reduction for the effect of terrain, benchmark elevation and latitude were employed for static gravity data. Topographic effects are corrected for using an automated algorithm based on dense circular zones (34 zones from 1 m to 60 km radius, 864 compartments in total), similar to Hammer zones, around the individual benchmarks [*Hammer*, 1939]. SRTM data was used for up to 20 km away from survey benchmarks, and a ten-time-subsampled terrain model was used for the far field. Terrain density is among the most critical parameters for gravimetric data reduction. Material between the elevation range of the survey (3600 – 6000 m a.s.l.) are mostly Neogene and Quaternary volcanics with a volumetrically very inferior Ordovician low-grade metamorphic unit [*Kussmaul et al.*, 1977]. Measurements on selected samples from different outcrops suggest a density value of 2.4 g/cm^3 is appropriate and hence is used here for terrain and Bouguer slab corrections (this generates no significant correlation between topography and calculated local anomaly). A linear correlation between VGG and terrain correction suggest that, in the absence of topography, the VGG for this area differs lees than 3% from the theoretical value of -308 μGal m^{-1}, which is the value used in the reduction. Finally, latitude is corrected for using the standard gravity formula [*Moritz*, 1980]. Sixty additional regional gravity data points are introduced from other surveys [*Götze et al.*, 1996] to improve the aperture of the network when calculating a regional gravity trend.

6. Preliminary findings

The calculated local gravity anomaly shows that Uturuncu and other neighbouring volcanoes are centred over a local bowl-shaped area of relative low gravity with no apparent relation to the main Neogene volcanic systems (Figure 2). The local gravity minimum is seen on the benchmarks south east of Utuurncu between the Vilama and Guacha caldera systems. It is unclear whether this anomaly refers to either caldera or to the massif located between them. Other strong negative anomalies are seen beneath the eastern flank of Uturuncu volcano and below the eastern limit of the Las Lagunillas ignimbrite plateau, which extends to the location of the Soniquera and Lipez Range Quaternary volcanoes. West of Laguna Colorada shield another negative anomaly is detected. The presence of the APMB suggest the negative anomaly may be caused by the presence of partial melt, as has been suggested by Schilling et al. [2006].

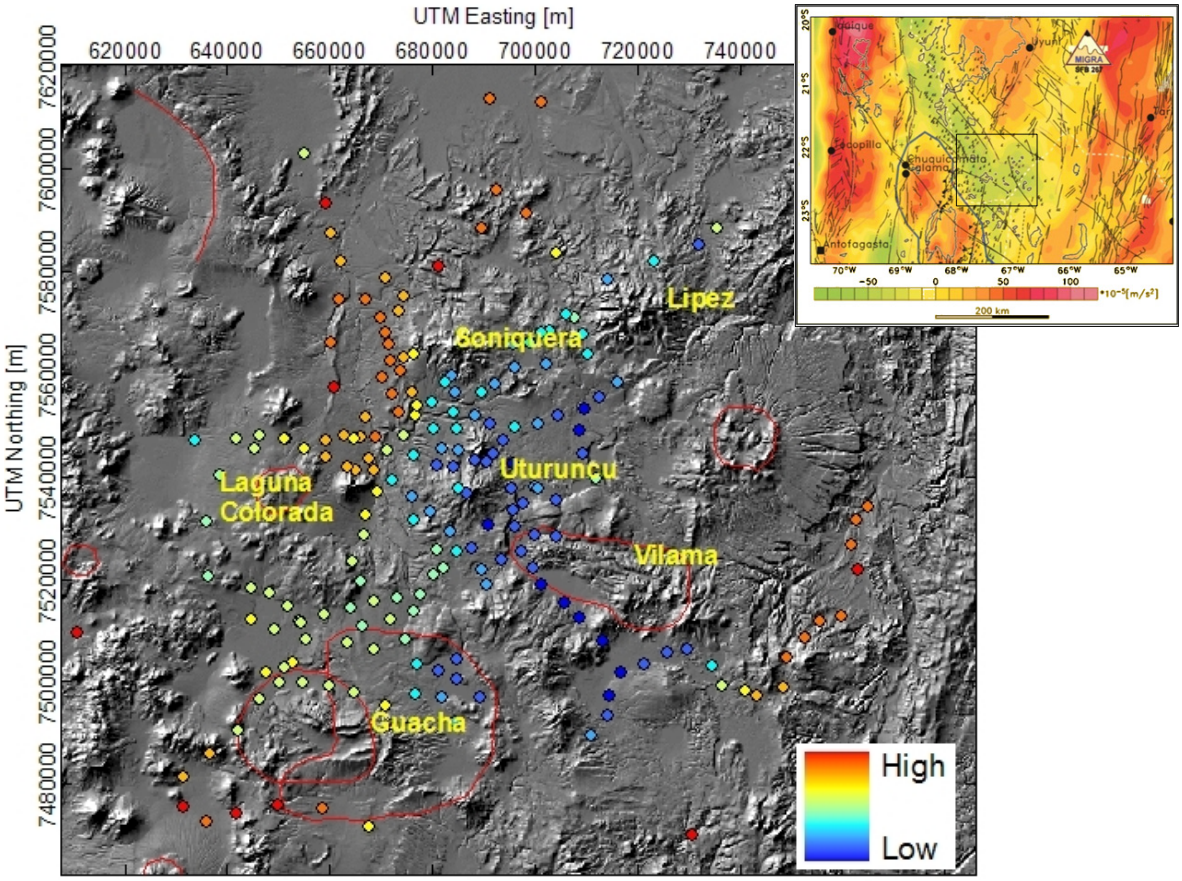

Figure 2. Calculated local gravity anomaly around Uturuncu volcano. The main volcanoes and caldera systems are shown. Inset shows the regional map of Götze et al. [1996].

The strongest positive anomalies are observed on the periphery of the survey, bounding the negative anomaly. A positive signal within the central part of the survey is observed northwest of Uturuncu. To the south this anomaly becomes a north-south oriented ridge that coincides with several outcrops of Ordovician rocks.

GPS measurements for the time-lapse surveys show consistent values with no significant ground deformation between the two campaigns. Microgravity measurements (shown in Figure 3) show a possible trend that becomes significant only when the standard error is used, and disappears for confidence intervals greater than 1σ.

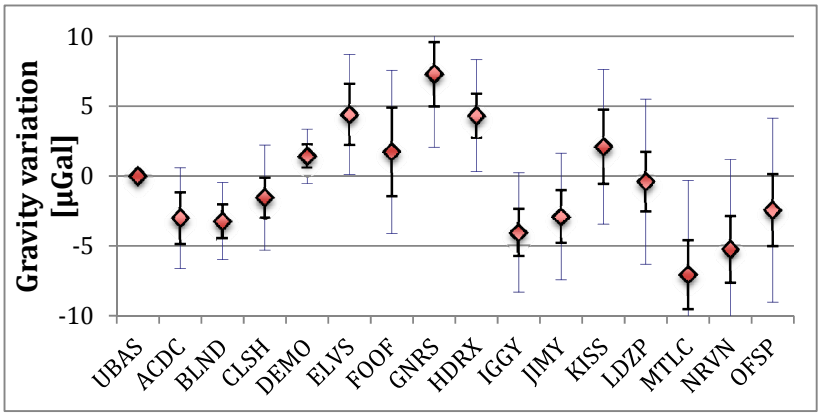

Figure 3. Microgravity variations measured in the first campaign. Black error bars represent the standard error while blue error bars are one standard deviation

7. Conclusions and recommendations

The gravity surveys provide first important insights on the subsurface structure and volcanic plumbing systems, and place some constraints on possible pluton growth beneath Uturuncu. The spatio-temporal variations of geophysical observables will provide further constraints. Questions remain as to the nature of the observed ground uplift in the past by InSAR studies. The surveys reported herein could have not been carried out without the equipment from NERC GEF Loans 910 & 928. The equipment used was optimal for the purpose of these surveys and will continue to be for future campaigns. Moreover, the quality of the data obtained exceeded expectations. Ideally a higher resolution DEM should be used for terrain corrections, but such data set does not yet exist. Several manuscripts are being drafted at the time of this writing to report the results from the static gravity surveys.

8. Resulting Publications and Communications

del Potro, R., Gottsmann, J., et al. Gravity signature of an active intrusion in the central Andes. Geophysical Research Abstracts Vol. 12, EGU2010-11220, 2010 EGU General Assembly.

del Potro, R., Gottsmann, J., et al. Gravity anomaly of a deep active intrusion beneath Uturuncu volcano in the central Andes. G23C-0849, 2010 Fall Meeting, AGU.

del Potro, R., Gottsmann, J., et al. Deep structure beneath Uturuncu volcano in the central Andes: Insights from new density anomaly models. EGU2011-8541, 2011 EGU General Assembly.

del Potro, R., Gottsmann, J., et al. 3D Density anomaly distribution in southern Bolivia. XXV IUGG General Assembly. *Accepted.*

We currently have three manuscripts in preparation that will be submitted for publication in 2011.

9. References

Camacho, A.G., et al. (2002), A 3-D gravity inversion tool based on exploration of model possibilities: Computer and Geosciences 28, 191-204.

Dehant, V., et al. (1999), Tides for a convective Earth, Journal of Geophysical Research-Solid Earth, 104(B1), 1035-1058.

Götze, H. J., et al. (1996), Group updates gravity database for central Andes, EOS Trans. AGU, 77(19), 181.

Hammer, S. (1939), Terrain corrections for gravimeter stations, Geophysics, 4, 184-194.

Kussmaul, S., et al. (1977), Volcanism and structure of southwestern Bolivia, Journal of Volcanology and Geothermal Research, 2(1), 73-&.

Moritz, H. (1980), Geodetic reference system 1980. Journal of Geodesy, Vol 54 (3), 395-405

Pritchard, M.E., and M. Simons. (2002), A satellite geodetic survey of large-scale deformation of volcanic centres in the central Andes, Nature, 418, 167-171

Salisbury, M.J., et al. (2010), 40Ar/39Ar chronostratigraphy of Altiplano-Puna volcanic complex ignimbrites reveals the development of a major magmatic province. Geological Society of America Bulletin, doi:10.1130/B30280.1

Schilling, F. R., et al. (2006), Partial Melting in the Central Andean Crust: a Review of Geophysical, Petrophysical, and Petrologic Evidence. In: O Oncken G Chong G Franz P Giese H-J Goetze VA Ramos MR Strecker P Wigger ed(s). The Andes, Active Subduction Orogeny. Berlin, Springer

Sparks, R. S. J., et al. (2008), Uturuncu volcano, Bolivia: Volcanic unrest due to mid-crustal magma intrusion. American Journal of Science, 308, 727-769.

APPENDIX - Site positions [UTM zone 19S]

CPREF Base

Site	Northing	Easting	Elevation	Site	Northing	Easting	Elevation
UBAS	7547174.77	633715.14	4458.7				
BQ1	7541744.62	663534.26	4487.1	CTRL-E	7526181.65	687674.25	4763.9
BQ2	7515803.37	668640.64	4639.9	CTRL-SM	7553661.27	676998.09	4245.6
BQ3	7533586.35	695712.75	4777.36	CTRL-I	7546677.05	693804.62	4477.0
BQ4	7556290.07	683898.93	4475.8	CTRL-FB	7544965.80	671219.89	4183.09
CTRL-A	7547999.42	646547.49	4866.0	CTRL-J	7550231.76	700508.47	4669.8
CTRL-B	7528520.12	666833.84	4304.4	CTRL-K	7537658.66	695532.60	4555.5
CTRL-C	7513058.73	658923.21	4583.5	CTRL-L	7510808.45	666419.76	4714.2
CTRL-D	7522126.22	682120.72	4787.7	CTRL-DN	7518899.01	701269.30	4605.6
CTRL-G	7550363.86	691411.95	4493.8	QTNA	7545111.13	671139.90	4155.0
CTRL-H	7567910.87	671107.76	4168.7				
031302	7543656.14	659361.25	4667.3	031703	7508363.72	674687.87	4615.7
031303	7545415.87	655190.86	4754.9	032402	7536802.93	686821.11	6053.8
031304	7547280.01	651448.16	4843.0	032403	7537589.36	685252.31	5463.6
031702	7512253.21	671993.98	4629.0	032404	7541743.81	684346.74	4799.7
031306	7547429.04	642006.58	4793.2	032502	7556506.50	676043.71	4335.2
031307	7547165.87	633764.22	4459.9	032503	7560574.00	673980.35	4447.4
031310	7543628.28	667580.49	4260.3	032504	7563740.99	676413.26	4649.3
031312	7547679.85	669103.06	4169.5	032505	7563131.07	674464.04	4393.7
031313	7547747.25	665989.21	4238.0	032506	7562665.29	672048.95	4287.6
031314	7547898.07	662809.16	4379.5	032507	7559311.00	670216.28	4272.9
031315	7547044.21	659335.14	4555.1	032508	7556136.55	672197.39	4318.5
031402	7541136.03	664997.32	4464.6	032509	7552450.79	673502.06	4419.8
031403	7541329.31	668723.23	4254.7	032511	7552565.81	684185.51	4373.0
031404	7536848.46	669227.03	4281.4	032512	7551859.55	688483.70	4452.0
031405	7532533.65	667155.14	4264.4	032514	7546939.37	693816.20	4519.7
031407	7523565.18	664595.73	4758.6	032515	7544591.00	692028.20	4561.8
031409	7539345.62	672361.18	4292.6	032516	7542949.77	690612.89	4628.6
031410	7536008.94	676090.20	4467.5	032517	7543145.81	688376.74	4779.4
031411	7531602.80	676343.82	4487.4	032518	7545187.36	685259.86	4487.5
031412	7533242.51	679807.99	4588.9	032519	7549309.41	684852.28	4413.7
031502	7514428.01	664188.94	4608.8	032904	7565890.39	671495.34	4187.2
031504	7511758.12	654104.49	4448.3	032905	7570975.52	669961.92	4116.3
031505	7510360.98	649353.66	4435.9	032906	7574419.19	667069.51	4079.7
031506	7512066.91	644759.58	4435.9	032910	7575195.68	674638.27	4174.7
031508	7508268.01	655359.88	4443.9	032911	7572139.42	673529.37	4232.5
031509	7503808.94	652970.17	4454.6	033002	7551597.23	667097.52	4193.9
031510	7499749.93	650191.15	4461.5	033103	7530320.49	696308.92	4636.1
031511	7501802.54	647706.25	4436.6	033104	7528352.85	704249.33	4696.7
031512	7499865.26	654789.21	4471.7	033105	7528527.18	699967.44	4629.4

031513	7499138.21	659891.92	4507.6	033106	7525494.77	697320.52	4594.7
031603	7519495.72	666123.26	4659.4	033108	7530613.70	690892.92	4696.2
031605	7516501.43	673273.18	4704.5	033110	7523826.38	693473.60	4664.3
031606	7516946.58	677878.64	4723.1	033111	7522125.23	699597.14	4599.5
031607	7520889.20	680262.71	4761.8	033113	7507936.72	713321.60	4740.2
031609	7525261.61	684763.42	4750.0	033114	7512419.90	708841.26	4626.1
031611	7529279.05	683693.46	4703.1	033115	7515266.11	705986.31	4581.5
031612	7525827.96	680988.76	4769.6	040303	7534602.81	697781.25	4648.0
031614	7531584.43	676322.00	4487.2	040305	7537755.00	695328.13	4562.4
040306	7542522.44	695855.08	4530.1	040703	7506320.98	668772.11	4688.8
040310	7537737.60	700563.34	4627.7	040705	7507686.94	663395.27	4681.2
040404	7551789.46	704616.06	4631.5	040707	7513597.81	676319.44	4654.4
040405	7553210.78	709770.92	4585.6	040603	7519028.84	690762.92	4804.7
040406	7558321.77	716140.75	4797.9	041003	7559525.93	683999.80	4641.7
040407	7555430.64	712713.39	4665.8	041004	7558439.54	682573.28	4484.3
040409	7549519.28	696187.21	4624.9	041005	7556332.58	684519.81	4471.5
040504	7535362.22	704208.01	4646.5	041009	7548898.63	708636.89	4546.4
040505	7538076.59	699868.38	4634.9	041010	7544368.35	709460.06	4611.4
040602	7521723.68	689801.52	4699.3	041011	7539737.10	712040.00	4642.4